MOL PHARM

MOLECULAR PHARMACOLOGY

Transcriptional Response to Corticotropin-Releasing Factor in AtT-20 Cells

Pieter J. Peeters, Hinrich W. Göhlmann, Ilse Van den Wyngaert, Sigrid M. Swagemakers, Luc Bijnens, Stefan U. Kass, and Thomas Steckler

Johnson & Johnson Pharmaceutical Research and Development, Beerse, Belgium

Received April 1, 2004; accepted July 22, 2004

ABSTRACT

Corticotropin-releasing factor (CRF) plays a central role in the regulation of the hypothalamic-pituitary-adrenal axis, mediating endocrine and behavioral responses to various stressors. Two high-affinity receptors for CRF have been described. Although many of the intracellular signaling pathways activated by CRF have been studied extensively, our knowledge of transcriptional responses downstream of the CRF receptor 1 (CRFR1) is still limited. To elucidate gene networks regulated by CRF and CRFR1, we applied microarray technology to explore transcriptional response to CRF stimulation. Therefore, mouse pituitary-derived AtT-20 cells were exposed continuously to CRF either in the presence or absence of the specific CRFR1 antagonist R121919. Transcriptional responses to different treatments were studied in a time course ranging from 0.5 to 24 h. Microarray data were analyzed using classic microarray data analysis tools such as correspondence factor analysis, cluster analysis, and fold-change filtering. Furthermore, spectral map analysis was applied, a recently introduced unsupervised multivariate analysis method. A broad and transient transcriptional response to CRF was identified that could be blocked by the antagonist. This way, several known CRF-induced target genes and novel CRF responsive genes were identified. These include transcription factors such as cAMP-responsive element modulator ($7\times$ increased), secreted peptides such as cholecystokinin ($1.5\times$), and proteins involved in modulating intracellular signaling, such as regulator of G-protein signaling 2 ($11\times$). Up-regulation of many of these genes can be explained as negative feedback, attenuating CRF-activated pathways. In addition, spectral map analysis proved to be a promising new tool for microarray data analysis.

Corticotropin releasing factor (CRF), a 41-amino acid polypeptide, plays a central role in the regulation of the hypothalamic-pituitary-adrenal axis, mediating neuroendocrine, autonomic, and behavioral responses to various stressors. Hypothalamic neurons from the parvocellular part of the paraventricular nucleus release CRF into the hypophyseal portal system in response to stress, stimulating the secretion and biosynthesis of adrenocorticotropin (ACTH) from pituitary corticotrophs, subsequently leading to increased adrenal glucocorticoid release (Steckler, 2001). Two high-affinity receptors for CRF have been described, CRFR1 and CRFR2, both of which exist in several

splice variant forms (Dautzenberg et al., 2001). CRFR1 expression is abundant in the brain and pituitary and is limited in the periphery (Steckler and Holsboer, 1999). In contrast to CRFR1, the expression pattern of CRFR2 is discrete in the brain and more widespread in the periphery. The intracellular signaling pathways activated by CRF in the anterior pituitary have been studied extensively (Bilezikjian and Vale, 1983; Aguilera et al., 1988; Rossant et al., 1999). Activation of the receptor by CRF results in G_s-mediated stimulation of adenyl cyclase, leading to increased levels of intracellular cAMP (Stalla et al., 1988). These high levels of cAMP lead to the activation of the cAMP-dependent protein kinase A (PKA) (Litvin et al., 1984). In addition to augmenting the production of cAMP, it has been shown that CRF triggers a persistent mem-

ASPET

brane depolarization via PKA-dependent closure of K^+ channels (Lee and Tse, 1997). This membrane depolarization in turn activates Ca^{2+} entry through L-type and P-type voltage-gated Ca^{2+} channels and causes a continuous cytosolic Ca^{2+} concentration increase. As a result of this, exocytosis via secretion vesicles located near the plasma membrane is stimulated (Tse and Lee, 2000).

Increased cytosolic levels of cAMP and Ca^{2+} lead to the activation of several other downstream effectors of CRF receptors. In addition to the above-mentioned PKA, additional kinases such as Ca^{2+}/calmodulin-dependent kinase II and p42/p44 mitogen-activated kinases are activated upon stimulation with CRF. As a result, Ca^{2+}/cAMP response element-binding (CREB) protein transcription factor is phosphorylated, in turn regulating the transcription of genes containing the Ca^{2+}/cAMP response element (Rossant et al., 1999). Examples of such genes include *c-fos* (Boutillier et al., 1991), macrophage migration-inhibitory factor gene *Mif* (Waeber et al., 1998), and orphan nuclear receptors *Nur77* and *Nurr1* (Murphy and Conneely, 1997). For the latter, it has been shown recently that CRF signaling leads to the induction of Nur77/Nur1 mRNA through PKA- and Ca^{2+}/calmodulin-dependent kinase II-dependent mechanisms, whereas Nurr77 transactivation through phosphorylation is dependent on mitogen-activated protein kinase regulation (Kovalovsky et al., 2002).

In addition to intracellular protein kinases, Ca^{2+}, and cAMP, CRH receptors modulate a plethora of other important signaling molecules such as nitric-oxide synthase, guanylyl cyclase, Fas and Fas ligand, and procaspase-3 pathways and suppress activities of glycogen synthase kinase 3 and nuclear factor-κB (Cantarella et al., 2001; Kostic et al., 2001; Dermitzaki et al., 2002; Radulovic et al., 2003). It is not always clear whether these effects are mediated via the CRHR1 or the CRHR2 subtype. In the case of nitric-oxide synthase, it seems that the divergent effects of CRH on different cell lines can be explained by different expression of either subtype of its receptor (Cantarella et al., 2001). Along the same line, accumulating evidence suggests tissue-specific coupling to G proteins and activation of different signaling cascades. In some tissues, CRFR1 may couple to Gq and activate the phospholipase C-protein kinase C cascade (Grammatopoulos et al., 2000).

AtT-20 cells have been studied intensively as a cellular model of corticotrophs. As such, many of the important players of the signaling cascade downstream of CRFR1 have been identified and studied in this cell line. Although several aspects of CRFR1 signaling have been extensively studied, at a transcriptional level, our insight is limited. The aim of this study was to explore the transcriptional response to continuous CRF exposure in the mouse pituitary corticotroph-derived adenoma cell line AtT-20 at the genome level using oligonucleotide microarrays and quantitative PCR. We report on novel CRF-responsive genes that are transiently induced after CRF exposure, an induction that can be suppressed by a CRFR1-specific antagonist R121919. Many of the induced transcripts encode proteins that would exert a negative feedback on the CRFR1 signaling, possibly contributing to the transient nature of the induction. The use of spectral map analysis of microarray data revealed the presence of both time- and CRF-related effects in transcriptional responses to prolonged CRF exposure. Our results demonstrate the power of this projection method in microarray data analysis.

Materials and Methods

Cell Culture and Sample Preparation. AtT-20 cells were purchased from the American Type Culture Collection (Manassas, VA) and were maintained at 37°C in 5% CO_2 in humidified air in Dulbecco's modified Eagle's medium (Invitrogen, Carlsbad, CA) containing 10% fetal bovine serum, 5% horse serum, and 4.5 g/l D-glucose. For experiments, cells were seeded in 25-cm^2 flasks. The medium was replaced 48 h later, and cells were treated with either 0.1% DMSO, 1 μM ovine CRF (Sigma-Aldrich, St. Louis, MO) in DMSO, 1 μM R121919 (Neurocrine Biosciences, San Diego, CA) in DMSO, or 1 μM CRF + 1 μM R121919 in DMSO for 0, 0.5, 1, 2, 4, 8, and 24 h in fresh medium. The dose of 1 μM CRF was chosen because it was shown to induce maximal response in a transactivation assay in AtT-20 cells transfected with a luciferase reporter construct (data not shown). The incubation was stopped by aspirating the incubation medium and adding 3 ml of TRIzol (Invitrogen) for lysis of the cells. Total RNA was extracted using TRIzol according to the manufacturer's instructions. Total RNA (100 μg) was further purified using QIAGEN Rneasy kit (QIAGEN, Leusden, the Netherlands) with DNaseI treatment on column.

Microarray Hybridization. cRNA was prepared as follows. Reverse transcription was performed on 10 μg of total RNA for 1 h at 42°C using a T7-oligo(dT)$_{24}$-primer and SuperscriptII RT (Invitrogen). Second-strand cDNA synthesis was done for 2 h at 16°C using *Escherichia coli* DNA polymerase I, DNA ligase, and RNaseH (Invitrogen). After phenol-chloroform extraction using phase-lock gel (Eppendorf, Hamburg, Germany), in vitro transcription was performed for 6 h at 37°C using the Bioarray high-yield RNA transcript-labeling kit with Biotin-labeled ribonucleotides (Enzo Diagnostics, Farmingdale, NY). cRNA samples were purified on QIAGEN Rneasy columns followed by fragmentation for 35 min at 95°C. cRNA yields were between 50 and 100 μg. Samples were processed on GeneChips (Affymetrix, Santa Clara, CA). To check the quality of each sample, 5 μg of labeled cRNA was run on Test2 arrays. Actual experiments were performed on murine genome U74Av2a arrays containing probe sets interrogating approximately 12,000 full-length mouse genes and expressed sequence tag clusters from the UniGene database (Build 74). Hybridization was performed using 15 μg of cRNA for 16 h at 45°C under continuous rotation. Arrays were stained in Affymetrix Fluidics stations using streptavidin/phycoerythrin followed by staining with antistreptavidin antibody and a second streptavidin/phycoerythrin staining. Thereafter, arrays were scanned with a Agilent Laserscanner (Affymetrix), and data were analyzed with the Microarray Suite Software 5.0 (Affymetrix). No scaling or normalization was performed at this stage. Quality of the experiment was assessed from the percentages of present calls across all samples, which was on average 47.06 ± 2.45%. The cytoplasmic β-actin and glyceraldehyde-3-phosphate dehydrogenase 5′/3′ ratios were 1.10 ± 0.08 and 0.93 ± 0.05, respectively.

Data Analysis and Selection of Genes

Normalization. Genes that were called absent in all samples according to Affymetrix MAS 5.0 software ($p > 0.06$) were removed from further analysis. Raw intensities from each chip were log$_2$-transformed, and all data from the sample of one time point were quantile-normalized using the method described by Amaratunga and Cabrera (2001). After the group-wise quantile normalization, a second quantile normalization was carried out across the data of all samples. In essence, this alignment sets the average intensity of one array to the average measured across all arrays, compensating for array-to-array variations in hybridization, washing, and staining, ultimately allowing a reasonable comparison between arrays.

Correspondence Factor Analysis and Spectral Map Analysis. Correspondence factor analysis and spectral map analysis are special cases of multivariate projection methods that help to reduce the complexity (dimensions) of highly dimensional data (n genes versus p samples). In essence, these so-called unsupervised methods

allow the reduction of the complexity of large microarray data sets and provide means to visually inspect and thereby identify clusters of genes and/or subjects in the data. Projected data are typically displayed in a biplot combining genes and samples in the same plot. Multivariate projection methods are taken from a derived space with k orthogonal axes. These k axes are linear combinations of the p original measurements (intensities) on the n genes. The axes are constructed in such a way that the first axis lies in the direction (in the multivariate data space) with the largest variability and the last axis in the direction with the smallest variability. In conventional principal component analysis, the first axis (principal component) that maximizes the variability is often related to the size of the intensities. Clusters that can be identified from the first axis will simply differ in absolute size of the intensities. Correspondence factor analysis (CFA) was originally developed for contingency tables and in a sense decomposes the χ^2 statistic. Therefore, distances between objects in CFA have a χ^2 distribution. In spectral map analysis (SPM) of log-transformed data, the distances are proportional to ratios of genes or samples. In microarray data, we are mainly interested in contrasts and not in simple high or low intensities. For that reason, both CFA and SPM have the appropriate properties (double closure for CFA and double centering for SPM) that remove the size component from the data. CFA and SPM will look for contrasts in intensities between genes without the nuisance effect of the absolute values of the intensities. Microarray data tend to be more reliable with increasing intensity. Therefore, reintroduction of the size component via variable weighting proportional to the mean intensities of genes and samples is required. A biplot (Chapman et al., 2002) created by the first two axes displays the maximal separation of both the genes and the samples. Coinciding clusters of samples and genes on the biplot indicate the genes (signatures) that are responsible for the separation of the samples. Genes that are located in the general direction of a sample on the biplot should be looked at as potential signatures for the separation of that sample versus the others. Because in microarray data there is a large difference in row and column dimension, an asymmetric factor-scaling is recommended in constructing the biplot. This operation pulls the genes away from the center of the biplot while leaving the samples at their original places (Wouters et al., 2003). Both methods were carried out in R (version 1.6.1) using the functions described by Wouters et al. (http://users.pandora.be/luc.wouters/spm.htm). R is an open-source implementation of the statistical programming language S (http://www.r-project.org).

k-Means Clustering, Hierarchical Clustering, and Fold Change. Additional analysis based on k-means clustering, hierarchical clustering, and fold-change criteria was carried out using the OmniViz program (OmniViz, Maynard, MA). Gene expression fold differences for CRF, R121919, and CRF + R121919 treatments were calculated at each time point. For those calculations, signals at corresponding time points in DMSO-treated samples were used as controls to calculate ratios. k-Means clustering (by magnitude and shape, 79 clusters) was done on all log$_2$-transformed ratios. Using the numeric query tool, genes were selected that were 2-fold up- or down-regulated in any of the experiments. Of 6393 genes, 975 showed a 2-fold change in expression level in at least one of the experiments. Then, 846 genes were selected that were differentially expressed and present in at least one of the experiments. For those 846 genes, a subset view was created, and hierarchical clustering (by magnitude and shape, 29 clusters) was done on log$_2$-transformed ratios. Using the OmniViz Treescape view (Fig. 3), 88 genes showing a difference in expression after treatment with CRF compared with treatment with the antagonist were selected (see supplementary Table 1).

Quantitative RT-PCR. Microarray data were confirmed using real-time PCR analysis. First-strand cDNA synthesis was performed on 0.5 μg of total RNA using random hexamer primers and SuperscriptII RT (Invitrogen). Quantitative PCR was performed on an ABIPrism 7700 cycler (Applied Biosystems, Foster City, CA) using a Taqman PCR kit (Applied Biosystems). Serial dilutions of cDNA were used to generate standard curves of threshold cycles versus the logarithms of concentration for β-actin and the genes of interest (Table 1 shows sequences of primers) (Eurogentec, Seraing, Belgium). Other quantitative assays were obtained from Applied Biosystems (Nurr1, Mm00443056_m1; Nur77, Mm00439358_m1; Per1, Mm00501813_m1; Atf3, Mm00476032_m1; Fyn, Mm00433373_m1; Snk, Mm00446917_m1; Pim3, Mm00446876_m1; Ptprn, Mm00436138_m1; and Dusp1, Mm00457274_g1). A linear-regression line calculated from the standard curves allowed the determination of transcript levels in RNA samples from the different time points. RT-PCR for CRFR1 and CRFR2 was performed using Amplitaq (Applied

TABLE 1
Sequence of oligonucleotides used for quantitative PCR

ß-actin	
Forward	5′-CATCTTGGCCTCACTGTCCAC-3′
Probe	5′-TGCTTGCTGATCCACATCTGCTGGA-3′
Reverse	5′-GGGCCGGACTCATCGTACT-3′
c-fos	
Forward	5′-GGGAGGACCTTACCTGTTCGT-3′
Probe	5′-CACCAGGCTGTGGGCCTCAAGG-3′
Reverse	5′-CCAGATGTGGATGCTTGCAA-3′
CRF2	
Forward	5′-GGGAGAACAGAAGCGCCTG-3′
Probe	5′-AGAAGGGTGAGGATCCCCCAAATCAGAGT-3′
Reverse	5′-CCCTTGTTTCAATCACTCCCA-3′
CRF1	
Forward	5′-TTTCTGAACAGTGAGGTCCGC-3′
Probe	5′-CCGGAAGAGGTGGCGGCGA-3′
Reverse	5′-GGGCTCTGATGGAGTGCTTG-3′
Rgs2	
Forward	5′-TTGGAAGACCCGTTTGAGCTA-3′
Probe	5′-TCTTGCAGAATTCCTCTGCTCCTGGG-3′
Reverse	5′-TTTCTTGCCAGTTTTGGGCT-3′
Fgfr2	
Forward	5′-AGACTTCCATGGGAATGATAGCA-3′
Probe	5′-CCTCTCGTCCGGCAGCTGGC-3′
Reverse	5′-AATGTGTAAGCCGGGCAGAA-3′
Mig6	
Forward	5′-AATCCTTTGTCCAATACTGTACACACA-3′
Probe	5′-GAAAAATGCACTGATCTCCGCA-3′
Reverse	5′-GTATGAACTAAATGAAGGTTAAAACATGCT-3′
PI-3K	
Forward	5′-CCATGGTGCTTGTTAACGCTTT-3′
Probe	5′-CCCAACTTGTAGCTGGTAAAGCTTCA-3′
Reverse	5′-CCTGTCTACCTTCTGGTCTCCAA-3′
CREM	
Forward	5′-CTTGCTGATCGTCTGGAGAGTTT-3′
Probe	5′-TGCTGATGACCCTCCATTGTGA-3′
Reverse	5′-TTAACATTCCTGAGGTTGCAAGAA-3′
Pde4b	
Forward	5′-GCCGTGTGTATGGCTGCAT-3′
Probe	5′-CAGCCCCCAGGCCACTGTGG-3′
Reverse	5′-AGGAGGGATAACAGGTGCTGTGT-3′
CCK	
Forward	5′-CCTGGACCCCAGCCATAGA-3′
Probe	5′-AGCCCATGTAGTCCCGGTCACTTA-3′
Reverse	5′-TGCGCCGGCCAAAA-3′
CT	
Forward	5′-GCTTGGACAGCCCCAGATC-3′
Probe	5′-GGTACTCAGATTCCCACACCGCTT-3′
Reverse	5′-TGTGTGTACGTGCCCAGCAT-3′
NFIL3	
Forward	5′-GCGAGTTTGAAGGCATGCA-3′
Probe	5′-CTCTCTTCACCCGCCGATGCGAT-3′
Reverse	5′-CCATGTTTCTCCAGGTCAAAATG-3′
RAMP3	
Forward	5′-TGGCAGACTCGGCTTCTGT-3′
Probe	5′-TTTGCTTTGGCCACACCCTACCTGG-3′
Reverse	5′-CTGGTCGGGAGGACTTTGG-3′
Sgk	
Forward	5′-TGGACCAATGCCCCAGTT-3′
Probe	5′-TCAGTCAAAGCCGTTGGTGTTTTCATTG-3′
Reverse	5′-GCCCGTTTTATAGGTGACATTTTAA-3′

Biosystems) on a 9600 cycler (Applied Biosystems) with 35 cycles and annealing temperature of 55°C.

Results

c-fos Expression after CRF Exposure. Transcriptional response to continuous CRF exposure was studied in the CRFR1-expressing murine AtT-20 pituitary corticotroph-derived adenoma cell line in a time course ranging from 0.5 to 24 h. Although CRFR1 was readily detectable by RT-PCR, CRFR2 expression could not be discerned in AtT-20 cells (Fig. 1). To identify CRFR1-specific responses, cells were exposed to CRF either in the presence or absence of the specific CRFR1 antagonist R121919 (Heinrichs et al., 2002). To this end, cells were incubated in fresh culture medium containing either a maximal stimulatory concentration of 1 μM CRF (Xiong et al., 1995), 1 μM CRF in the presence of 1 μM of R121919, or 1 μM R121919 alone. Maximal stimulatory concentrations were used to enhance differences between CRF- and antagonist-treated samples. Transcriptional responses were followed over time, starting from 30 min until 24 h after administration. To assess treatment efficacy, c-fos mRNA levels were determined by quantitative PCR on RNA from the different treatments and time points before array experiments were carried out. In agreement with previous reports, exposure to CRF elicited a transient surge in c-fos transcription, with levels already decreasing after 30 min to 1 h (Fig. 2) (Boutillier et al., 1991). This response was almost completely suppressed in the presence of R121919. It is interesting to note that 0.1% DMSO induced c-fos expression; however, levels were between 5 and 10 times lower compared with CRF-induced expression.

Graphical Exploration of Array Data Using Projection Methods. All time points were analyzed on oligonucleotide microarrays interrogating expression levels of approximately 12,000 mouse genes and ESTs. Overall, analysis of the expression profiles at the different time points and different treatments was performed using multivariate projection methods such as SPM and CFA. In the SPM biplot
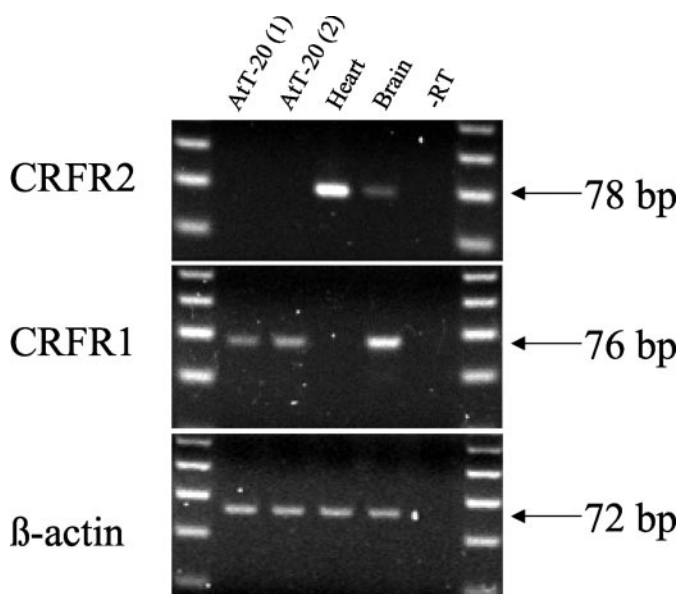

Fig. 1. Expression of CRFR1 and CRFR2 in AtT-20 cells. RT-PCR reactions were performed on two isolates of AtT-20 cells, mouse heart and mouse brain RNA, with primers specific for mouse CRFR1 and CRFR2. Both receptors are expressed in brain, whereas only CRFR2 is expressed in heart. As a control for RNA quality, primers for β-actin were used. bp, base pairs.

showing the first two principal components, samples seemed to be clustered more according to time point (Fig. 3A). This is exemplified by the genes that cluster with the samples. The gene with identifier 95632_f_at (mevalonate kinase) clustered together with samples isolated at 4 and 8 h. This implies that the gene is responsible for the separation of the 4- and 8-h samples from the other time points. Indeed, high levels of expression of the mevalonate kinase gene (95632_f_at) are observed 4 and 8 h after the beginning of the exposure, irrespective of treatment (Fig. 3A, left inset). At the opposite side of the biplot, the RIKEN cDNA 4930429H24 gene with identifier 96494_at is located together with samples exposed for 0.5, 1, and 24 h, indicating that this gene is highly expressed at these time points (Fig. 3A, right inset). The first two principal components of SPM clearly indicate that progressing time accounts for most of the observed changes in gene expression. When applying CFA, a similar clustering by time point was observed when plotting the first two principal components. However, in contrast to the SPM biplot, CRF-treated samples seemed to be separated from the other treatments at the corresponding time point. This is mainly the case for the early time points (1–4 h). More striking is the SPM biplot of the first versus the third principal component, in which all CRF-treated samples are separated from other samples (Fig. 3B). This points toward an overall difference in expression for CRF-treated samples compared with the other treatments. After 8 h of exposure, this overall difference diminishes. It is interesting to note the observation that R121919 treatment suppresses CRF effects, as indicated by the clustering of CRF + R121919 samples with either untreated samples or compound-only–treated samples. The clear separation of the time and CRF exposure effect was not observed in the CFA, even when looking at all principal components, demonstrating a clear difference between the algorithms. One important feature of both correspondence analysis and spectral map analysis is that they allow the identification of genes that contribute to differences in samples. As indicated in the CFA biplot, some genes are clustered together with the CRF-treated sample. As shown in the inset in Fig. 3C, the transcription factor JunB (102362_i_at) is readily up-regulated at 0.5 h of exposure to CRF with a maximum at 1 h. As a consequence, this gene clusters together with the CRF 1-h–treated sample. Likewise, cAMP-responsive element modulator (CREM) CREM-ICER (100533_s_at) and cholecystokinin (96055_at) are clustered with the CRF-treated samples at 2 and 4 h of exposure, respectively. In this way SPM and, to a lesser extent, CFA allowed the identification of genes specifically induced by CRF (Table 2).

Cluster and Fold-Change Difference Analysis. Other methods of identifying genes regulated by CRF include k-means clustering and fold-change difference analysis. Because of the obvious influence of time, expression measurements were analyzed relative to those observed in the corresponding time point in DMSO-treated control samples. Regulated genes were defined as those showing a greater than 2-fold change in transcript levels at any one time point. Using the OmniViz Treescape view, 88 genes that showed a difference in expression after treatment with CRF compared with treatment with the antagonist were selected (see *Materials and Methods*). Of the 88 genes, 17 were "early responders", showing at least a 2-fold change already after 30 min treatment with CRF; 48 genes
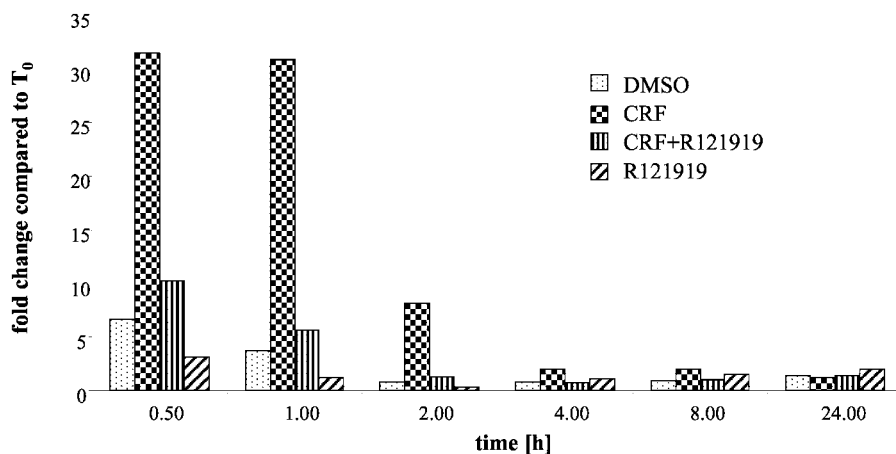
Fig. 2. Normalized *c-fos* expression after CRF treatment. c-fos mRNA levels were assessed by quantitative RT-PCR normalized against β-actin mRNA levels in AtT-20 cells continuously exposed to DMSO, 1 μM CRF, 1 μM CRF + R121919, or 1 μM R121919 in a time course ranging from 30 min to 24 h.
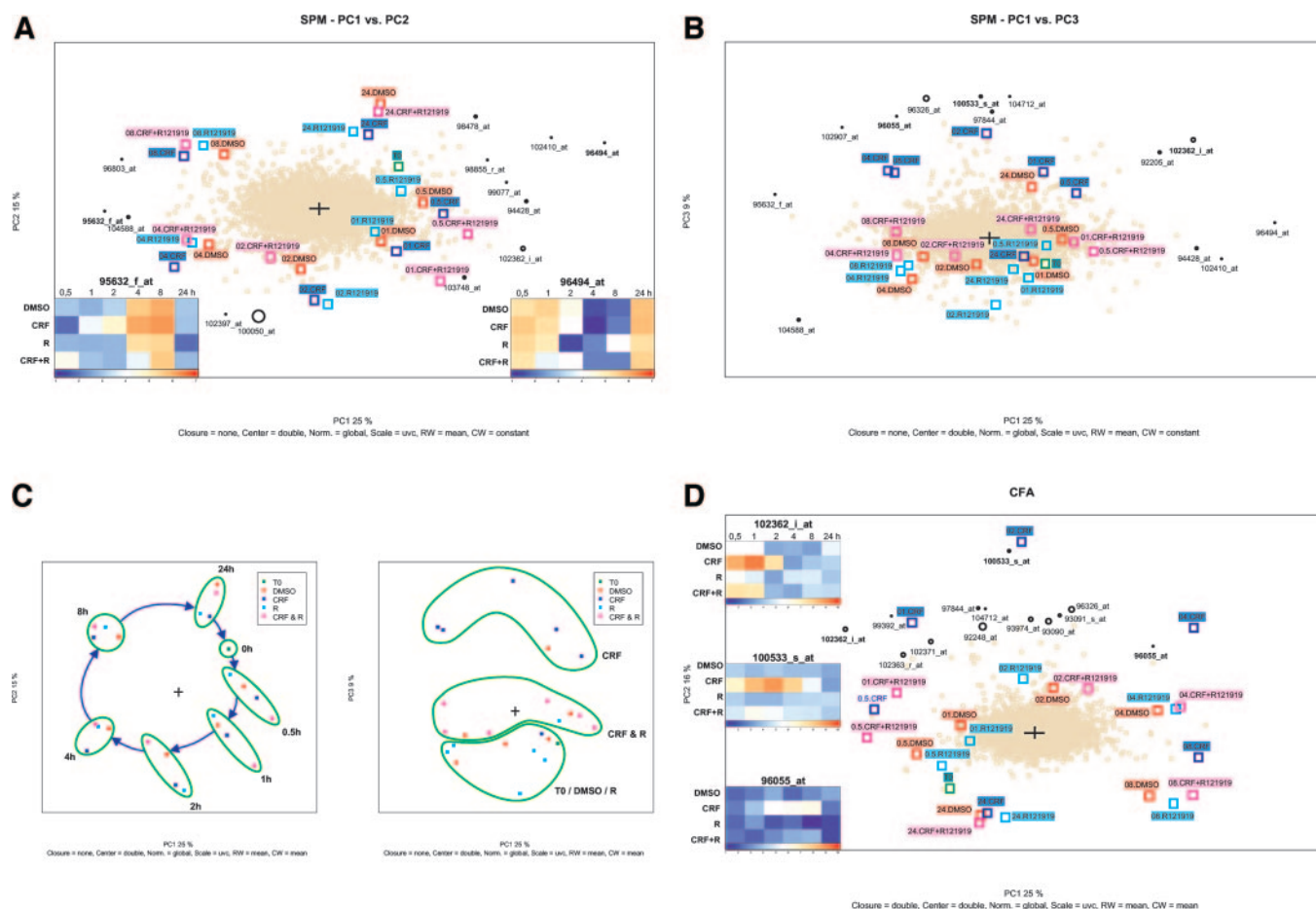
Fig. 3. Spectral map and correspondence analysis of microarray data. A, first two principal components (PC) of the weighted SPM applied on normalized microarray data for all time points and treatments. On the spectral map, squares depict different samples, and circles depict genes (size of circle corresponds to intensity). Distances between squares are a measure for similarity between samples. A positive association of a gene with a given sample (i.e., an up-regulation of that gene in that particular sample) results in the positioning of the gene and sample on a common line through the centroid (depicted by a cross). Genes contributing significantly (measured by their distance form the centroid) to difference between samples are annotated with their Affymetrix identifier (http://www.affymetrix.com/analysis/netaffx) (Table 2 contains annotation). The first two PCs identified time as the major discriminator between the samples. Inserted heat maps (insets) show representative genes (indicated in boldface type in biplot) that are maximally induced either after 4 and 8 h or at 0.5, 1, and 24 h, corresponding to their position on the biplot. B, biplot of first and third PCs. The third PC identifies the specific CRF effect on AtT-20 cells over time. C, summary views on the first three dimensions of spectral map, showing how this technique identified time and CRF effects in the microarray dataset. D, CFA applied on the same data as shown in A. The interpretation of the CFA output is similar to that of SPM. In addition to time, CFA identified the effect of CRF exposure as most prominent in the early time points (1–4 h). Inserted heat maps show representative genes that are maximally induced after either 1, 2, or 4 h of exposure to CRF, corresponding to their position on the map.

were "intermediate responders", responding between 1 and 2 h after start of the treatment, and 23 genes were "late responders", showing a response after 2 h or more (Fig. 4). These responses were all suppressed by the CRFR1 antagonist R121919 (Fig. 4). Among the early responders were known players in the pathways downstream of the CRFR1 such as the transcription factors Nurr1, Nurr77, and Jun-B, validating the assay. It is interesting that 50 of the 88 genes which were identified using this arbitrary fold-change criterion were also identified in the unsupervised spectral map and correspondence factor analysis. A direct comparison of the genes identified by the different methods is shown in Table 2.

TABLE 2
Genes identified on SPM and CFA biplots

| Probe Set ID	Gene Symbol	Gene Name
SPM PC1vsPC2		
100050_at	Idb1	Inhibitor of DNA binding 1
102362_i_at	Junb	Jun-B oncogene
102397_at	Cbfa2t3h	Core-binding factor, runt domain, α subunit 2; translocated to 3 homolog
102410_at	Hs3st1	Heparin sulfate (glucosamine) 3-O-sulfotransferase 1
103748_at	4933407C03Rik	RIKEN cDNA 4933407C03 gene
104588_at	1810073K19Rik	RIKEN cDNA 1810073K19 gene
94428_at	Ilvbl	ilvB (bacterial acetolactate synthase)-like
95632_f_at	Mvk	Mevalonate kinase
96494_at	4930429H24Rik	RIKEN cDNA 4930429H24 gene
96803_at	Gbe1	Glucan (1,4-α-), branching enzyme 1
98478_at	Ccng2	Cyclin G2
98855_r_at		Weak similarity to melanoma-associated chondroitin sulfate proteoglycan 4
99077_at	Thra	Thyroid hormone receptor α
SPM PC1vsPC3		
100533_s_at	Crem	cAMP-responsive element modulator
102362_i_at	Junb	Jun-B oncogene
102410_at	Hs3st1	Heparin sulfate (glucosamine) 3-O-sulfotransferase 1
102907_at	C820004H04Rik	RIKEN cDNA C820004H04 gene
104588_at	1810073K19Rik	RIKEN cDNA 1810073K19 gene
104712_at	Myc	Myelocytomatosis oncogene
92205_at		Moderate similarity to insulin receptor substrate 2
94428_at	Ilvbl	ilvB (bacterial acetolactate synthase)-like
95632_f_at	Mvk	Mevalonate kinase
96055_at	Cck	Cholecystokinin
96326_at	Tat	Tyrosine aminotransferase
96494_at	4930429H24Rik	RIKEN cDNA 4930429H24 gene
97844_at	Rgs2	Regulator of G-protein signaling 2
CFA		
100533_s_at	Crem	cAMP responsive element modulator
102362_i_at	Junb	Jun-B oncogene
102363_r_at	Junb	Jun-B oncogene
102371_at	Nr4a1	Nuclear receptor subfamily 4, group A, member 1
104712_at	Myc	Myelocytomatosis oncogene
92248_at	Nr4a2	Nuclear receptor subfamily 4, group A, member 2
93090_at	Fgfr2	Fibroblast growth factor receptor 2
93091_s_at	Fgfr2	Fibroblast growth factor receptor 2
93974_at	1300002F13Rik	RIKEN cDNA 1300002F13 gene
96055_at	Cck	Cholecystokinin
96326_at	Tat	Tyrosine aminotransferase
97844_at	Rgs2	Regulator of G-protein signaling 2
99329_at	Abcc1	ATP-binding cassette, sub-family C
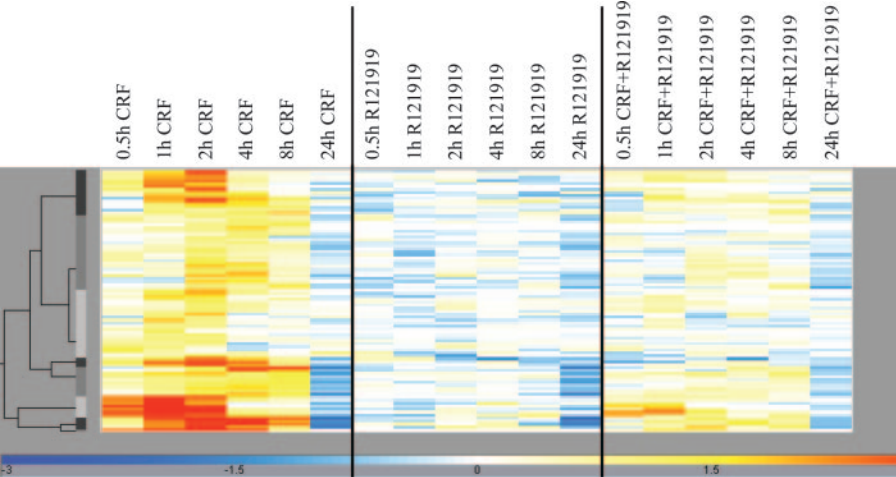
Fig. 4. Heat map of selected genes affected by CRF exposure. A heat map depicting 88 genes that are changed upon CRF treatment as identified by a combination of cluster analysis and fold-change criteria (for a list of the 88 genes, see supplementary Table 1). Values were calculated by dividing the intensity of each sample by the intensity of the DMSO sample at the corresponding time point. These calculated ratios are converted into a color ramp on a $\log_2$ scale. In this way, the different timing of induction of expression becomes apparent. Genes showing a 2-fold change after 30 min of treatment with CRF were called "early responders", "intermediate responders" show a change after 1 to 2 h of treatment, and "late responders" show a response after 2 h or more.

Genes Induced by CRF Exposure. Remarkable novel players identified using methods outlined above include transcription factors [e.g., hairy/enhancer-of-split related 1, nuclear factor regulated by interleukin 3 (NFIL3), CREM, and prostate-specific ets transcription factor], receptor and channel regulators [e.g., Ras-related GTP-binding protein (Gem) and receptor (calcitonin) activity-modifying protein 3 (RAMP3)], secreted peptides (e.g., calcitonin, cholecystokinin), and proteins involved in intracellular signaling [e.g., regulator of G-protein signaling 2 (Rgs2), cAMP-specific phosphodiesterase 4B (Pde4b), and the regulatory subunit phosphatidylinositol 3-kinase, p85]. Other regulated genes comprise period homolog Per1, fibroblast growth factor receptor 2 (Fgfr2), serum/glucocorticoid-regulated kinase, and serum-inducible kinase (Fig. 5). All responders identified according to the above-mentioned criteria were up-regulated after exposure to CRF. This induction was transient, and nearly all of the induced genes returned to baseline after 4 to 8 h. Many of the induced transcripts encode proteins that would exert a negative feedback on the CRFR1 signaling (e.g., Pde4, Rgs2, and CREM), possibly contributing to the transient nature of the induction. In addition to this negative feedback, other mechanism such as desensitization of CRFR1

through phosphorylation and internalization contribute to the transient nature of transcriptional induction (Hauger et al., 2000; Dautzenberg et al., 2002). In this respect, it is interesting to note that challenge with CRF quickly down-regulates CRFR1 mRNA in rat pituitary cells (Pozzoli et al., 1996). Although array experiments did not reveal obvious alterations in CRFR1 mRNA, quantitative PCR showed an increase in CRFR1 mRNA in AtT-20 cells exposed to 1 μM CRF after 1 (3.4-fold) and 2 (2.2-fold) h of exposure (Fig. 6). It is interesting that even in the presence of R121919, an up-regulation of CRFR1 mRNA is observed, although it is less pronounced and with some delay to the response in CRF-treated samples.

Quantitative PCR. Confirmation of microarray data were carried out using quantitative PCR on the same samples used for hybridization experiments and furthermore on an independent experiment. Levels of regulation and the time course identified by microarray experiments were in agreement with those observed by quantitative PCR. For those genes that have been tested, levels of induction compared with the untreated sample are shown in Fig. 5. A comparison between the time course identified by microarray and quantitative PCR is shown in Fig. 7, demonstrating the regulation of Rgs2.
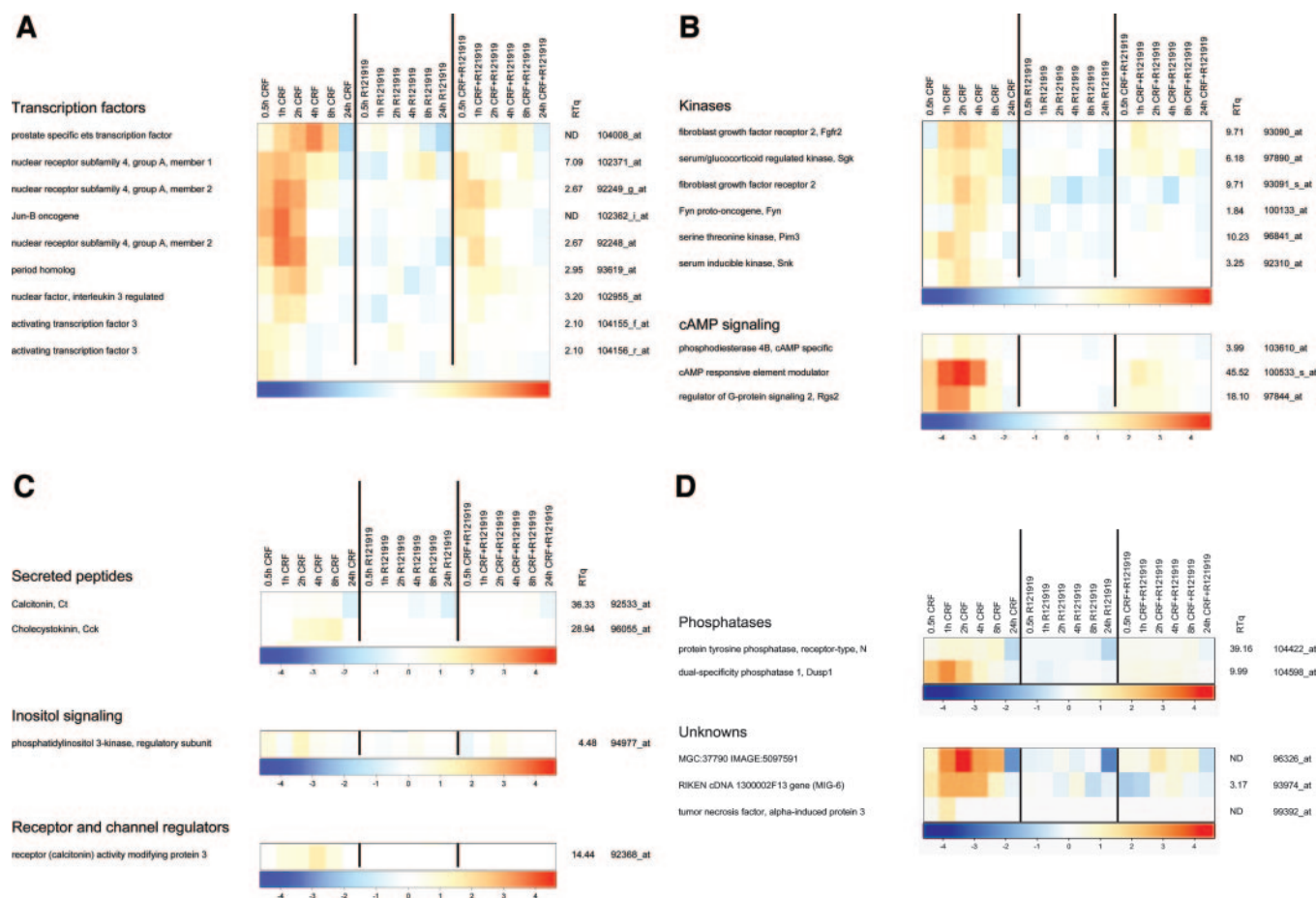

Fig. 5. Overview of regulated pathways. Overview of a selection of genes induced by CRF grouped by pathway or function. Values were calculated by dividing the intensity of each sample by the intensity of the DMSO sample at the corresponding time point. These calculated ratios are converted into a color ramp on a log$_2$ scale and depicted in a heat map. Next to the heat maps, the maximal fold change over all time points as detected by quantitative PCR is shown for each gene tested. These PCR data were obtained on a repeated experiment. For an overview of all quantitative PCR data, see supplementary Table 2. At the right Affymetrix identifiers for each gene are depicted. ND, not done.

Discussion

To identify transcriptional pathways downstream of the CRFR1, we applied oligonucleotide microarray analysis on AtT-20 cells exposed to CRF and the CRFR1-specific antagonist R121919. A transient induction of negative regulators of CRFR1 signaling was observed. Several previously unknown CRF-inducible genes, were identified such as *Rgs2*, *Pde4b,* and *CREM*. The use of microarray data to explore the mechanism of action of a compound requires efficient analysis tools that allow for the rapid identification of specific signatures in gene expression across different samples. Projection methods allow this type of graphical exploration by reducing complex multidimensional data to a two-dimensional subspace in which samples and genes are plotted together, such as principal component analysis and CFA (Alter et al., 2000; Hastie et al., 2000; Holter et al., 2000; Fellenberg et al., 2001). SPM was recently introduced as an alternative unsupervised multivariate projection method. Weighted SPM outperforms principal component analysis and is at least as powerful as CFA in finding clusters in the samples as well as in identifying genes related to these clusters (Wouters et al., 2003). When applying SPM and CFA to our data set, we identified exposure time to treatment as an important discriminator between the different samples. Synchronization of cell cycle in these cultures induced by the addition of new medium and serum could possibly account for this phenomenon, although the accumulation of metabolites and progressing cell-culture conditions are additional contributing factors. Besides time, SPM identified an effect of CRF treatment in the early time points. These effects of CRF are in agreement with activation of several second messengers, such as cAMP and Ca^{2+}, upon stimulation with CRF. Moreover, all of these effects were blocked by the CRFR1-specific antagonist R121919. Some of the transcriptional responses can be explained by the phosphorylation of CREB and the subsequent transcription of genes downstream of cAMP-responsive elements. These elements have been found in the promoters of *Per1*, *Nurr1*, *CREM-ICER*, and *c-fos*. Furthermore the kinetic profile of the induction of these genes corresponds with the observed maximal transcription rate by CREB after 0.5 h of initial cAMP formation. The induction of *CREM-ICER* constitutes a negative feedback mechanism in attenuating transcriptional response to cAMP (Lamas et al., 1997). The reported induction of *CREM-ICER* in response to acute stress in the intermediate lobe of the pituitary gland is of particular interest. Mice deficient for *CREM-ICER* show a long-term increase of β-endorphin levels, suggesting that *CREM-ICER* induction may be involved in the modulation of gene expression in response to stress (Mazzucchelli and Sassone-Corsi, 1999). Our results suggest that *CREM-ICER* is directly involved in the modulation of CRF signaling, and as a result, ablation of *CREM-ICER* could lead to an altered response to stress signals.

Another novel putative negative-feedback regulator of CRF signaling is Rgs2. We identified two single Ca^{2+}/cAMP response element motifs in the promoter of the human *RGS2* gene, providing a possible explanation for the early response behavior of this gene upon stimulation with CRF. In support of our findings is a recent report showing that both phosphoinositide signaling and cAMP induce a rapid and transient increase in *RGS2* mRNA in human astrocytoma and neuroblastoma cells (Zmijewski et al., 2001). The Rgs2 protein is a selective inhibitor of $G_{q\alpha}$ function (Heximer et al., 1997). It has been shown that Rgs2 reduces odorant-elicited cAMP production, not by acting on $G\alpha$ but by directly inhibiting the activity of adenyl cyclase type III (Sinnarajah et al., 2001). Although *Rgs2* was originally identified as an immediate early-response gene in activated T lymphocytes, studies in *Rgs2*-deficient mice indicate that it also plays a role in the modulation of stress-related behavior, because these mice show increased anxiety and aggression (Oliveira-Dos-Santos et al., 2000).

The induction of *Pde4b*, encoding an enzyme responsible for hydrolysis of cAMP (particularly in nerve and immune cells), can also be categorized as negative feedback, directly attenuating the cAMP signal.

Another important second messenger generated upon stimulation with CRF is Ca^{2+}. It has been shown that CRF triggers a steady-state depolarization-stimulated extracellular Ca^{2+} entry via voltage-gated Ca^{2+} channels and increases intracellular Ca^{2+} concentration through release from inositol 1,4,5-triphosphate–sensitive Ca^{2+} pools (Tse and Lee, 2000). This leads to the secretion of ACTH. Wortmannin has been shown to inhibit both calcium-independent
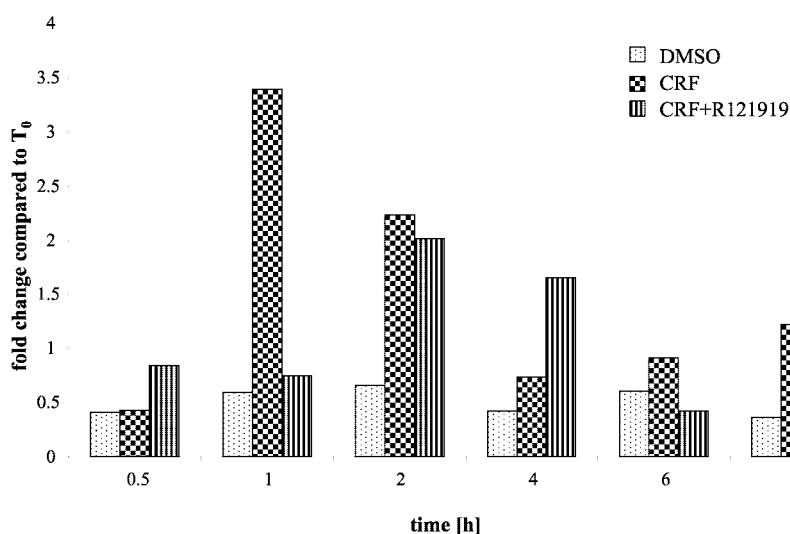
Fig. 6. Induction of CRFR1 mRNA by CRF in AtT-20 cells. Quantitative PCR results with CRFR1-specific primers. Induction is calculated in comparison with levels observed in AtT-20 cells before any treatment.

and -stimulated secretion from permeabilized AtT-20 cells, indicating a role for phosphatidylinositol-3 kinase (PI-3K) in determining the size of the readily releasable pool of ACTH (Wilson and Guild, 2001). The p85 regulatory α subunit of PI-3K is up-regulated in CRF-treated AtT-20 cells. This up-regulation of the regulatory unit might constitute an attenuation of PI-3K activity. In addition to its role as second messenger, intracellular Ca^{2+} has also been shown to play a critical role in regulating gene expression. The regulation of NFIL3/E4BP4 by calcineurin/NFAT and CaM kinase signaling (Nishimura and Tanaka, 2001), accounting for an in-

crease in NFIL3 mRNA levels upon CRF treatment, is interesting. In B lymphocytes, expression of NFIL3 is induced by interleukin 3 through both the Raf–mitogen-activated protein kinase and phosphatidylinositol 3-kinase pathways. In this cell type, NFIL3 inhibits apoptosis in synergy with Bcl-xL–dependent pathways (Kuribara et al., 1999). Our data suggest a role for NFIL3 in the prevention of apoptosis in AtT-20 cells, further supporting a cytoprotective effect of CRF by suppression of proapoptotic pathways (Radulovic et al., 2003).

CRF is the most efficacious ACTH secretagogue. Several other prepropeptide mRNAs were found to be up-regulated after CRF administration, such as cholecystokinin (CCK) and calcitonin (CT). The up-regulation of RAMP3 is particularly interesting in this respect. RAMPs control the transport and glycosylation of the calcitonin receptor-like receptor. In the case of RAMP3, it has been shown that together with calcitonin receptor-like receptor, it generates an adrenomedullin receptor (McLatchie et al., 1998). Up-regulation of this gene might play a role in regulating the responsiveness of AtT-20 cells to adrenomedullin after CRF exposure. In addition, the regulation of RAMP3 could influence responses to other extracellular stimuli such as CRF, because it is known that RAMPs might regulate other G-coupled receptors, such as vasoactive intestinal polypetide receptor and parathyroid receptor (Christopoulos et al., 2003).

Although CCK is secreted by AtT-20 cells, induction of its expression by CRF has not been reported previously (Beinfeld, 1992). Interaction between CCK and CRF has been studied intensively and demonstrated in panic attacks, depression, anxiety, and gastric emptying (Coskun et al., 1997; Geracioti et al., 1999; Kellner et al., 2000). Most of these experiments point toward a role for CRF in mediating the central effects of CCK. Our data indicate that additionally, CRF might function as a CCK secretagogue.

In agreement with previous reports, we could find an up-regulation of CRFR1 mRNA after prolonged CRFR1 exposure (Iredale et al., 1996). It is tempting to speculate that this up-regulation compensates for the loss of receptor at the surface after internalization and restores responsiveness of the cells. An interesting observation is the similar up-regulation with a shift in time in the cells treated with CRF in the presence of the antagonist. This suggests that these receptor complexes also are internalized.

In conclusion, we have unraveled part of the corticotropin-releasing hormone receptor-1–activated gene network and have identified several novel targets of this signaling cascade. In addition, we have demonstrated the power of spectral map analysis for microarray data exploration.
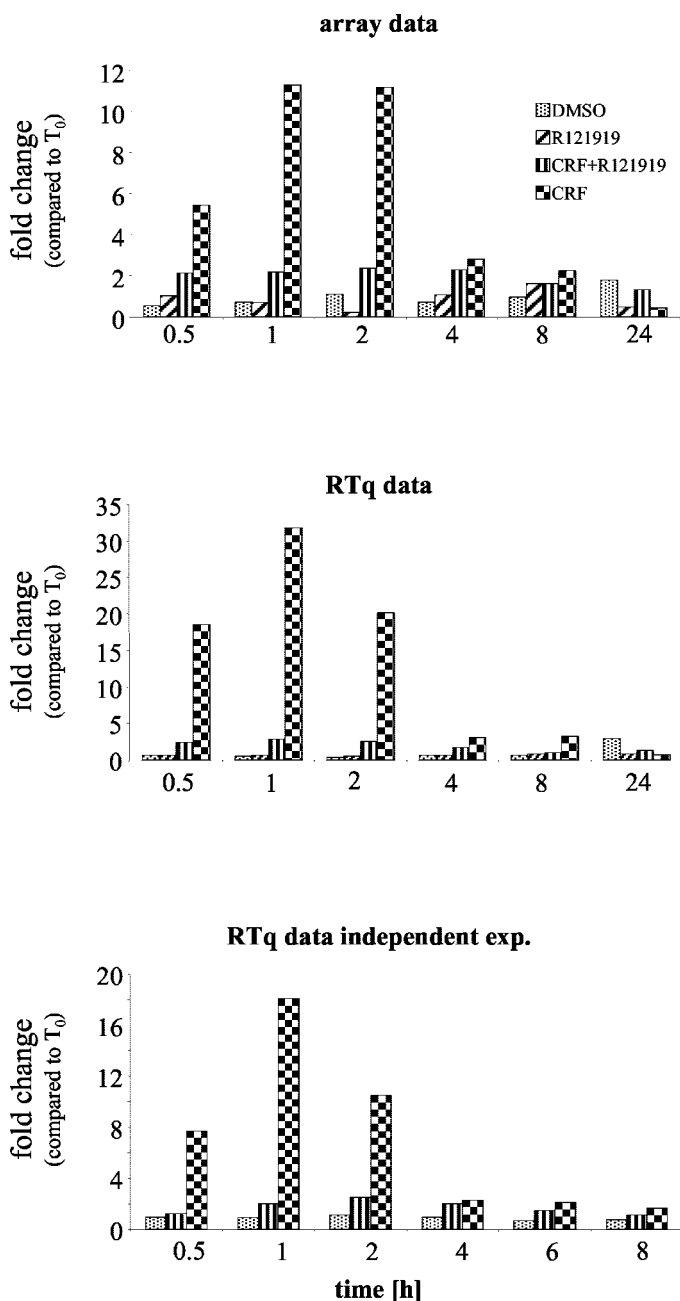

Fig. 7. Induction of Rgs2 mRNA by CRF in AtT-20 cells. Induction is calculated in comparison with levels observed in AtT-20 cells before any treatment. Top, array data obtained for *Rgs2* are shown. Bottom, levels of Rgs2 mRNA as measured by quantitative RT-PCR on the same samples as used for array experiments and as measured in an independent experiment.

References

Aguilera G, Abou Samra AB, Harwood JP, and Catt KJ (1988) Corticotropin releasing factor receptors: characterization and actions in the anterior pituitary gland. *Adv Exp Med Biol* **245:**83–105.

Alter O, Brown PO, and Botstein D (2000) Singular value decomposition for genome-wide expression data processing and modeling. *Proc Natl Acad Sci USA* **97:**10101–10106.

Amaratunga D and Cabrera J (2001) Analysis of data from viral DNA microchips. *J Am Stat Assoc* **96:**1161–1170.

Beinfeld MC (1992) CCK mRNA expression, pro-CCK processing and regulated secretion of immunoreactive CCK peptides by rat insulinoma (RIN 5F) and mouse pituitary tumor (AtT-20) cells in culture. *Neuropeptides* **22:**213–217.

Bilezikjian LM and Vale WW (1983) Glucocorticoids inhibit corticotropin-releasing factor-induced production of adenosine 3′,5′-monophosphate in cultured anterior pituitary cells. *Endocrinology* **113:**657–662.

Boutillier AL, Sassone-Corsi P, and Loeffler JP (1991) The protooncogene C-fos is

MOL PHARM

MOLECULAR PHARMACOLOGY

aspet

induced by corticotropin-releasing factor and stimulates proopiomelanocortin gene transcription in pituitary cells. *Mol Endocrinol* **5:**1301–1310.

Cantarella G, Lempereur L, Lombardo G, Chiarenza A, Pafumi C, Zappala G, and Bernardini R (2001) Divergent effects of corticotropin releasing hormone on endothelial cell nitric oxide synthase are associated with different expression of CRH type 1 and 2 receptors. *Br J Pharmacol* **134:**837–844.

Chapman S, Schenk P, Kazan K, and Manners J (2002) Using biplots to interpret gene expression patterns in plants. *Bioinformatics* **18:**202–204.

Christopoulos A, Christopoulos G, Morfis M, Udawela M, Laburthe M, Couvineau A, Kuwasako K, Tilakaratne N, and Sexton PM (2003) Novel receptor partners and function of receptor activity-modifying proteins. *J Biol Chem* **278:**3293–3297.

Coskun T, Bozkurt A, Alican I, Ozkutlu U, Kurtel H, and Yegen BC (1997) Pathways mediating CRF-induced inhibition of gastric emptying in rats. *Regul Pept* **69:**113–120.

Dautzenberg FM, Kilpatrick GJ, Hauger RL, and Moreau J (2001) Molecular biology of the CRH receptors—in the mood. *Peptides* **22:**753–760.

Dautzenberg FM, Wille S, Braun S, and Hauger RL (2002) GRK3 regulation during CRF- and urocortin-induced CRF1 receptor desensitization. *Biochem Biophys Res Commun* **298:**303–308.

Dermitzaki E, Tsatsanis C, Gravanis A, and Margioris AN (2002) Corticotropin-releasing hormone induces Fas ligand production and apoptosis in PC12 cells via activation of P38 mitogen-activated protein kinase. *J Biol Chem* **277:**12280–12287.

Fellenberg K, Hauser NC, Brors B, Neutzner A, Hoheisel JD, and Vingron M (2001) Correspondence analysis applied to microarray data. *Proc Natl Acad Sci USA* **98:**10781–10786.

Geracioti TD Jr, Ekhator NN, Nicholson WE, Arndt S, Loosen PT, and Orth DN (1999) Intra- and inter-individual correlations between cholecystokinin and corticotropin-releasing hormone concentrations in human cerebrospinal fluid. *Depress Anxiety* **10:**77–80.

Grammatopoulos DK, Randeva HS, Levine MA, Katsanou ES, and Hillhouse EW (2000) Urocortin, but not corticotropin-releasing hormone (CRH), activates the mitogen-activated protein kinase signal transduction pathway in human pregnant myometrium: an effect mediated via r1α and r2β CRH receptor subtypes and stimulation of Gq-proteins. *Mol Endocrinol* **14:**2076–2091.

Hastie T, Tibshirani R, Eisen MB, Alizadeh A, Levy R, Staudt L, Chan WC, Botstein D, and Brown P (2000) "Gene shaving" as a method for identifying distinct sets of genes with similar expression patterns. *Genome Biol* **1:**1–21.

Hauger RL, Smith RD, Braun S, Dautzenberg FM, and Catt KJ (2000) Rapid agonist-induced phosphorylation of the human CRF receptor, type 1: a potential mechanism for homologous desensitization. *Biochem Biophys Res Commun* **268:**572–576.

Heinrichs SC, De Souza EB, Schulteis G, Lapsansky JL, and Grigoriadis DE (2002) Brain penetrance, receptor occupancy and antistress in vivo efficacy of a small molecule corticotropin releasing factor type I receptor selective antagonist. *Neuropsychopharmacology* **27:**194–202.

Heximer SP, Watson N, Linder ME, Blumer KJ, and Hepler JR (1997) RGS2/G0S8 is a selective inhibitor of Gqα function. *Proc Natl Acad Sci USA* **94:**14389–14393.

Holter NS, Mitra M, Maritan A, Cieplak M, Banavar JR, and Fedoroff NV (2000) Fundamental patterns underlying gene expression profiles: simplicity from complexity. *Proc Natl Acad Sci USA* **97:**8409–8414.

Iredale PA, Terwilliger R, Widnell KL, Nestler EJ, and Duman RS (1996) Differential regulation of corticotropin-releasing factor1 receptor expression by stress and agonist treatments in brain and cultured cells. *Mol Pharmacol* **50:**1103–1110.

Kellner M, Wiedemann K, Yassouridis A, Levengood R, Guo LS, Holsboer F, and Yehuda R (2000) Behavioral and endocrine response to cholecystokinin tetrapeptide in patients with posttraumatic stress disorder. *Biol Psychiatry* **47:**107–111.

Kostic TS, Andric SA, and Stojilkovic SS (2001) Spontaneous and receptor-controlled soluble guanylyl cyclase activity in anterior pituitary cells. *Mol Endocrinol* **15:**1010–1022.

Kovalovsky D, Refojo D, Liberman AC, Hochbaum D, Pereda MP, Coso OA, Stalla GK, Holsboer F, and Arzt E (2002) Activation and induction of NUR77/NURR1 in corticotrophs by CRH/CAMP: involvement of calcium, protein kinase A and MAPK pathways. *Mol Endocrinol* **16:**1638–1651.

Kuribara R, Kinoshita T, Miyajima A, Shinjyo T, Yoshihara T, Inukai T, Ozawa K, Look AT, and Inaba T (1999) Two distinct interleukin-3-mediated signal pathways, Ras-NFIL3 (E4BP4) and Bcl-XL, regulate the survival of murine pro-B lymphocytes. *Mol Cell Biol* **19:**2754–2762.

Lamas M, Molina C, Foulkes NS, Jansen E, and Sassone-Corsi P (1997) Ectopic ICER expression in pituitary corticotroph AtT20 cells: effects on morphology, cell cycle and hormonal production. *Mol Endocrinol* **11:**1425–1434.

Lee AK and Tse A (1997) Mechanism underlying corticotropin-releasing hormone (CRH) triggered cytosolic Ca²⁺ rise in identified rat corticotrophs. *J Physiol (Lond)* **504:**367–378.

Litvin Y, PasMantier R, Fleischer N, and Erlichman J (1984) Hormonal activation of the CAMP-dependent protein kinases in AtT20 cells. Preferential activation of protein kinase I by corticotropin releasing factor, isoproterenol and forskolin. *J Biol Chem* **259:**10296–10302.

Mazzucchelli C and Sassone-Corsi P (1999) The inducible cyclic adenosine monophosphate early repressor (ICER) in the pituitary intermediate lobe: role in the stress response. *Mol Cell Endocrinol* **155:**101–113.

McLatchie LM, Fraser NJ, Main MJ, Wise A, Brown J, Thompson N, Solari R, Lee MG, and Foord SM (1998) RAMPs regulate the transport and ligand specificity of the calcitonin-receptor-like receptor. *Nature (Lond)* **393:**333–339.

Murphy EP and Conneely OM (1997) Neuroendocrine regulation of the hypothalamic pituitary adrenal axis by the Nurr1/Nur77 subfamily of nuclear receptors. *Mol Endocrinol* **11:**39–47.

Nishimura Y and Tanaka T (2001) Calcium-dependent activation of nuclear factor regulated by interleukin 3/adenovirus E4 promoter-binding protein gene expression by calcineurin/nuclear factor of activated T cells and calcium/calmodulin-dependent protein kinase signaling. *J Biol Chem* **276:**19921–19928.

Oliveira-Dos-Santos AJ, Matsumoto G, Snow BE, Bai D, Houston FP, Whishaw IQ, Mariathasan S, Sasaki T, Wakeham A, Ohashi PS, et al. (2000) Regulation of T cell activation, anxiety and male aggression by RGS2. *Proc Natl Acad Sci USA* **97:**12272–12277.

Pozzoli G, Bilezikjian LM, Perrin MH, Blount AL, and Vale WW (1996) Corticotropin-releasing factor (CRF) and glucocorticoids modulate the expression of type 1 CRF receptor messenger ribonucleic acid in rat anterior pituitary cell cultures. *Endocrinology* **137:**65–71.

Radulovic M, Hippel C, and Spiess J (2003) Corticotropin-releasing factor (CRF) rapidly suppresses apoptosis by acting upstream of the activation of caspases. *J Neurochem* **84:**1074–1085.

Rossant CJ, Pinnock RD, Hughes J, Hall MD, and McNulty S (1999) Corticotropin-releasing factor type 1 and type 2alpha receptors regulate phosphorylation of calcium/cyclic adenosine 3′,5′-monophosphate response element-binding protein and activation of P42/P44 mitogen-activated protein kinase. *Endocrinology* **140:**1525–1536.

Sinnarajah S, Dessauer CW, Srikumar D, Chen J, Yuen J, Yilma S, Dennis JC, Morrison EE, Vodyanoy V, and Kehrl JH (2001) RGS2 regulates signal transduction in olfactory neurons by attenuating activation of adenylyl cyclase III. *Nature (Lond)* **409:**1051–1055.

Stalla GK, Stalla J, Huber M, Loeffler JP, Hollt V, von Werder K, and Muller OA (1988) Ketoconazole inhibits corticotropic cell function in vitro. *Endocrinology* **122:**618–623.

Steckler T (2001) The molecular neurobiology of stress–evidence from genetic and epigenetic models. *Behav Pharmacol* **12:**381–427.

Steckler T and Holsboer F (1999) Corticotropin-releasing hormone receptor subtypes and emotion. *Biol Psychiatry* **46:**1480–1508.

Tse A and Lee AK (2000) Voltage-gated Ca²⁺ channels and intracellular Ca²⁺ release regulate exocytosis in identified rat corticotrophs. *J Physiol (Lond)* **528:**79–90.

Waeber G, Thompson N, Chautard T, Steinmann M, Nicod P, Pralong FP, Calandra T, and Gaillard RC (1998) Transcriptional activation of the macrophage migration-inhibitory factor gene by the corticotropin-releasing factor is mediated by the cyclic adenosine 3′,5′- monophosphate responsive element-binding protein CREB in pituitary cells. *Mol Endocrinol* **12:**698–705.

Wilson ML and Guild SB (2001) Effects of wortmannin upon the late stages of the secretory pathway of AtT-20 cells. *Eur J Pharmacol* **413:**55–62.

Wouters L, Göhlmann HW, Bijnens L, Kass SU, Molenberghs G, and Lewi PJ (2003) Graphical exploration of gene expression data: a comparative study of three multivariate methods. *Biometrics* **59:**1133–1141.

Xiong Y, Xie LY, and Abou-Samra AB (1995) Signaling properties of mouse and human corticotropin-releasing factor (CRF) receptors: decreased coupling efficiency of human type II CRF receptor. *Endocrinology* **136:**1828–1834.

Zmijewski JW, Song L, Harkins L, Cobbs CS, and Jope RS (2001) Second messengers regulate RGS2 expression which is targeted to the nucleus. *Biochim Biophys Acta* **19:**201–211.

Address correspondence to: Dr. Pieter Peeters, Johnson and Johnson Pharmaceutical Research and Development, a Division of Janssen Pharmaceutica N.V., Turnhoutseweg 30, 2340 Beerse, Belgium. E-mail: ppeeter3@prdbe.jnj.com